Electron–ion coincidence measurements: The neutral dissociation cross section for CF_4

L. Mi and R. A. Bonham
Department of Biological, Chemical, and Physical Sciences, Illinois Institute of Technology, Chicago, Illinois, 60616

(Received 2 September 1997; accepted 24 October 1997)

Pulsed electron beam time-of-flight measurements of the electron energy loss spectrum of CF_4 at scattering angles of 28°, 45°, 71°, 112°, and 135° were made at impact energies of 22, 25, and 34 eV in coincidence with positive ions. The angular-dependent elastic, total dissociation, ionization, and neutral dissociation cross sections were measured. The data were integrated over electron energy loss for each scattering angle. These angular dependent data were then fitted with various analytic functions and integrated over angle to obtain individual total cross sections. All cross-section data were placed on an absolute scale by matching to total cross-section measurements reported in the literature. The angular-dependent elastic cross section and the integrated cross sections for elastic and total dissociation were found to be in good agreement with literature values. Values obtained for the neutral dissociation cross section agree with the difference between previous separate measurements of total dissociation by Winters and Inokuti and total ionization by Bruce and Bonham, but are inconsistent with those of the direct measurements of Sugai *et al.* The total ionization cross sections agree to within the experimental uncertainties with literature values. © *1998 American Institute of Physics.* [S0021-9606(98)01905-9]

I. INTRODUCTION

Carbon tetrafluoride is one of the most widely used components of feed gas mixtures employed for a variety of plasma-assisted material-processing applications. It has no stable excited states and the neutral and ionic fragments of the CF_4 molecule, generated in the low temperature plasma by low energy electron (<100 eV) impact, are ideal sources of reactive species. To understand the plasma etching process using CF_4 one needs to know all types of electron impact cross sections, especially the electron impact neutral dissociation cross section (i.e., dissociation of a molecule into neutral fragments only).[1,2] So far only two direct methods[3,4] and two indirect methods[5,6] for measuring it have been reported. Unfortunately, the total neutral dissociation cross sections inferred from the indirect measurement[5,7] for CF_4 are in serious disagreement with the direct measurements.[3] This paper describes the use of a newly reported indirect method[8] to obtain this important quantity. The results reported here should settle the dispute as to the correct neutral dissociation cross section for the important etching gas CF_4.

A pulsed electron beam time-of-flight experiment is reported in which five electron impact energy loss spectra, all at different scattering angles, were recorded simultaneously and in coincidence with all positive ions produced in the experiment. The data can be used to determine the angular dependence of total, elastic, total inelastic, ionization (total and partial), and the sum of neutral dissociation and excitation cross sections. By use of appropriate analytic functions the angular scattering data for each cross-section type can be integrated over angle and energy loss to obtain the corresponding integrated cross section.

II. EXPERIMENT

A. Method

A detailed description of the apparatus and the experimental procedure has been given elsewhere.[8,9] Briefly, an electron pulse of 5 ns full width at half-maximum height (FWHM), containing electrons of a known energy, intersects an effusive gas jet target containing the molecules to be studied. The region defined by the intersection of the two beams is located between two ion extraction lenses backed by flight tubes leading to microchannel plate detectors. The cylindrical axes of these two flight tubes are 180° apart and perpendicular to the trajectory of the unscattered electron pulse. A plane containing the trajectory of the unscattered electron pulse and perpendicular to the cylindrical axes of the two ion extraction tubes contains five electron flight tubes, located nominally at scattering angles of 28°, 45°, 71°, 112°, and 135°, that are 27 cm long with two 18-mm-diam microchannel plates in a chevron configuration at the end to register scattered and ejected electrons. The signals from each of the five electron detectors were routed, after suitable processing, to separate stops in a LeCroy 4208 multichannel time to digital converter (TDC), that had been started when the electron-impact pulse was generated. After the scattered electrons had all entered the shielded electron flight tubes, the ion extraction grids were activated and the positive ion flight times were recorded. The opposing ion detector biased for negative ion extraction was not used in this experiment. The experimental repeat rate was about 25 kHz, and the total ion count rate was less than 500 Hz. A typical spectrum is shown in Fig. 1.

The electron–ion coincidence data were used to establish the instrumental efficiency for ion detection for each electron detector. An example of the instrumental efficiency,

 0021-9606/98/108(5)/1910/5/$15.00

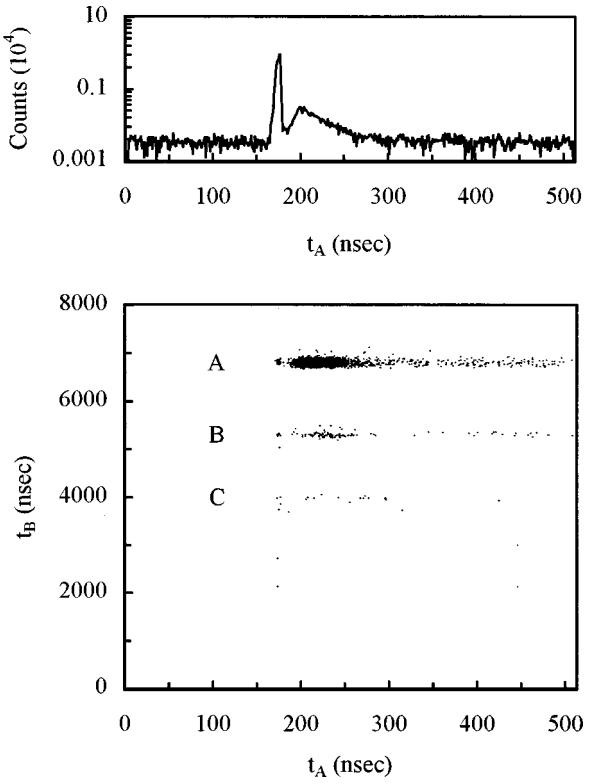

FIG. 1. Typical electron–ion coincidence and electron energy loss spectra. These spectra were recorded at a scattering angle of 45° and electron impact energy of 34 eV. The upper figure is the electron energy loss spectrum with total counts on the vertical axis and electron flight time on the horizontal axis. The dominant sharp peak is the elastic line while the weak features to its right constitute the inelastic scattering. The lower figure is a plot of the ion flight time on the vertical axis and electron flight time on the horizontal axis for electron–ion coincident events. The line labeled A corresponds to the partial ionization channel $e+CF_4 \rightarrow 2e+CF_3^+ +F$, B labels the partial ionization channel $e+CF_4 \rightarrow 2e+CF_2^+ +2F$ (or F_2) while C labels the partial ionization channel $e+CF_4 \rightarrow 2e+CF^+ +3F$ (or F_2+F). Accidental coincidences have been estimated and have been subtracted out.

$\epsilon(t)$, for one of the ion detectors is shown in Fig. 2. In principle, the efficiency should be the same for each detector but differences were observed,[8] especially for the 28° detector which had a higher count rate from electrons scattered

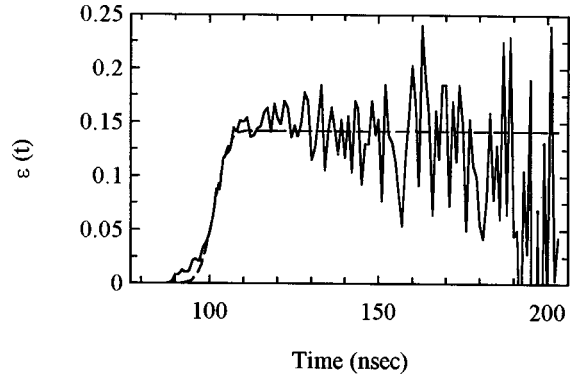

FIG. 2. The ion detection efficiency, $\varepsilon(t)$, as a function of electron flight time for the detector at 45° and an electron impact energy of 34 eV. The increasing noise with increasing electron flight time is due to increasing statistical uncertainty from the decreasing number of observed events. The smooth dashed curve is the theoretical efficiency based on the deconvolution procedure in Ref. 6.

from apertures and the chamber walls, and hence a lower efficiency for ion detection. Because there can be slight differences in the viewing solid angle of each detector and in the angular alignment, there is no guarantee that each detector sees a predictable region of the scattering volume. To circumvent this problem, we collected data for He at incident energies of 25, 30, and 50 eV and used the experimental data of Brunger *et al.*[10] to obtain a matching constant for each scattering angle.[8] The fact that the matching constants were relatively independent of electron impact energy was taken as validation of the procedure. The constant values reported in Ref. 8 were also used in this work.

In the case of the angular-dependent elastic scattering, a superposition of Legendre polynomials of the form

$$\left(\frac{d\sigma}{d\Omega}\right)_{\text{elastic}} = \sum_{i=0}^{4} a_i P_i(\cos\,\theta) \tag{1}$$

was employed to fit the data, which yielded integrated cross sections:

$$\sigma_{\text{elastic}} = 2\pi \int_0^{\pi} d\theta\, \sin\,\theta \left(\frac{d\sigma}{d\Omega}\right)_{\text{elastic}} = 4\pi a_0 . \tag{2}$$

Note that $\sin\theta$ in the definition of the integrated cross section acts as a weighting function which reduces the influence of both small ($\sim 0°$) and large angle ($\sim 180°$) data. With only five measurements, the integrated cross section is sensitive to the choice of fitting functions. We tested the sensitivity of the present total elastic cross sections to the form of fit by repeating the procedure using the shape of the extensive experimental data of Boesten *et al.*[11] as a guide. The sensitivity test fitting function used was

$$\left(\frac{d\sigma}{d\Omega}\right)_{\text{elastic}} = b_0 + b_1\theta^1 + b_2\theta^{1.5} + b_3\theta^2 + b_4\theta^{2.5}. \tag{3}$$

For the elastic integrated cross section, the two different fits showed an agreement of 10% with the recommended elastic integral cross section of Christophorou *et al.*[2] An example of the result at the impact energy of 25 eV is presented in Fig. 3, where the solid curve is the Legendre fit and the dashed curve is the fit following Eq. (3). Since the elastic scattering dominates the total scattering, these same forms were used to fit the total scattering cross sections.

In the case of the inelastic cross sections, we chose to break up the cross section for any excitation *not resulting in ionization of the parent or a fragment* into two parts. The cross section for any process which results in dissociation into neutral fragments only will be referred to as the neutral dissociation cross section, while the cross section for excitation not resulting in dissociation will be called the excitation cross section. In the case of CF_4, spectral emission data and the absence of a parent peak in the mass spectrum argue that all types of electronic excitation lead to dissociation, and hence the excitation cross section in the sense used here vanishes.[1,2]

The determination of the angular dependence of the total dissociation, neutral dissociation, and ionization contribu-

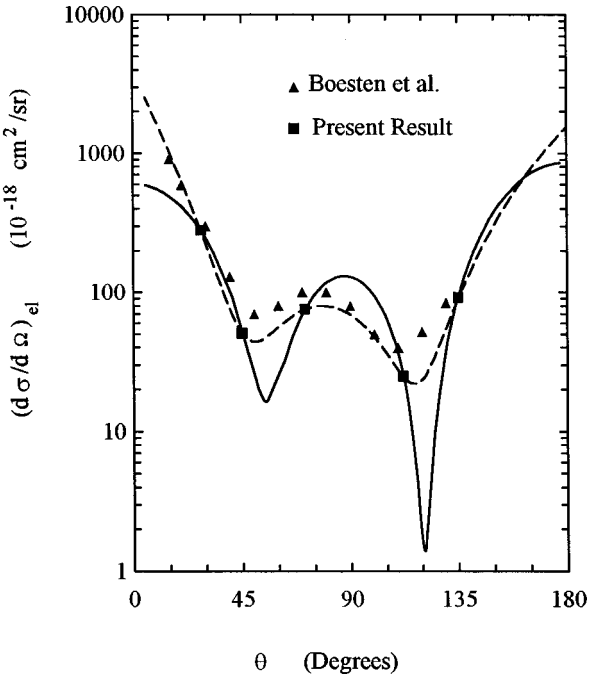

FIG. 3. The angular dependence of the elastic cross section for the electron impact energy of 25 eV. The triangles are values interpolated from the data of Boesten *et al.*, Ref. 11. The squares are the data points obtained in this study. The solid curve is the Legendre fit following Eq. (1) while the dashed curve is the fit following Eq. (3).

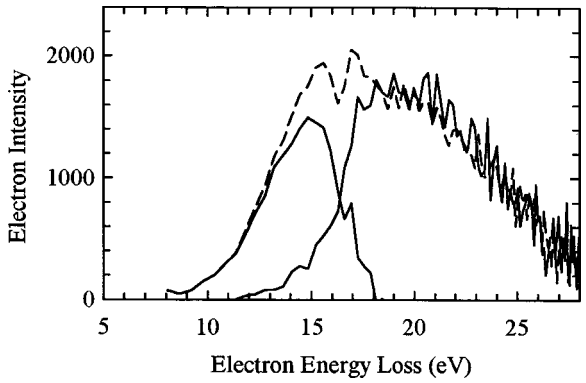

FIG. 4. Electron energy loss spectra at a scattering angle of 45° and electron impact energy of 34 eV. The dotted curve is the total inelastic scattering while the solid curve on the right is the ion coincidence data which has been placed on the same scale by means of the ion detection efficiency. The solid curve on the left is the difference between the former two curves and represents the contribution from neutral dissociation.

tions proved to be more difficult because of the paucity of our data and the absence of angular data from other laboratories (i.e., this is the first known attempt to measure these quantities for CF_4). Our data were first transformed from a time-of-flight scale to an energy loss scale. The ionization contribution was placed on the same relative scale as the electron energy loss spectrum by means of the detector efficiency and subtracted out to obtain the relative contribution due to neutral dissociation. A key assumption is that a region exists at sufficiently high energy loss where only ionization contributes to the inelastic scattering. This assumption was checked at an angle of 45° in the case of CF_4 in Ref. 6 by collecting data on the rare gases. An example of results of this procedure for a single impact energy and scattering angle is shown in Fig. 4.

For low electron impact energies, it has been shown[8] that an expansion in Legendre polynomials of the form

$$\left(\frac{d\sigma}{d\Omega}\right)_{\text{inelastic}} = a_0 P_0(\cos\,\theta) + \sum_{n=1}^{N} a_{j_n} P_{j_n}(\cos\,\theta) \qquad (4)$$

provides a good means for representing the three different inelastic angular distributions (total dissociation, ionization, and neutral dissociation). To test the sensitivity of the integrated cross section to the choice of Legendre expansion, we repeated the fitting procedure with $N=2$, 3, or 4 and the order of Legendre functions, j_n, varied over the range from 1 to 10. Only those least-squares fits to the experimental data which yielded a R-squared value (i.e., the ratio of the model sum of squares to the total sum of squares) of larger than 0.95 and had positive definite cross sections (''good'' fits) were considered as candidates for estimating the integrated cross sections. The integrated cross sections, σ_{dissoc}, σ_{ion}, or $\sigma_{\text{neut.dissoc.}}$, are given by the simple formula $4\pi a_0$ in all cases. All ''good'' fits were found to contain P_0, P_2, and P_4 terms. Typically the coefficients of these three terms were stable and were bigger than those of other terms in the cases of four- ($N=3$) and five-term ($N=4$) fits. In fact, the deviation from the average integrated cross section of all fits was

TABLE I. Coefficients a_i of three-term Legendre fits (P_0, P_2, P_4).

Process	Energy (eV)	a_0 (10^{-18} cm^2/sr)	a_2 (10^{-18} cm^2/sr)	a_4 (10^{-18} cm^2/sr)	$4\pi a_0$ (10^{-16} cm^2)
Neutral dissociation	22	3.44	4.42	8.83	0.43
	25	5.14	7.36	11.27	0.65
	34	6.09	7.43	9.26	0.77
Ionization	22	6.37	6.17	13.30	0.80
	25	10.57	13.21	25.34	1.33
	34	15.42	18.81	32.54	1.94
Total dissociation	22	9.86	10.66	22.43	1.24
	25	15.85	21.45	38.49	1.99
	34	21.71	26.47	42.10	2.73

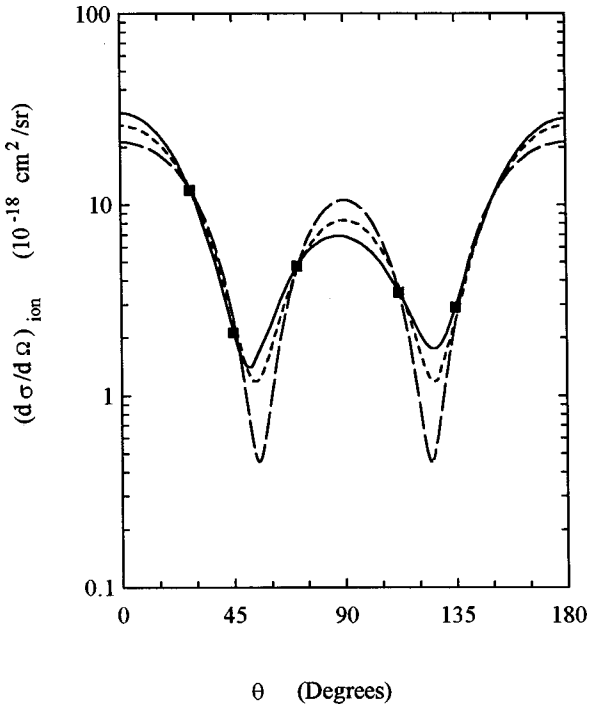

FIG. 5. The angular dependence of scattered electrons producing ionization at 22 eV. The solid curve is a representative five-term Legendre fit (P_0,P_2,P_4,P_5,P_6), the long dashed curve is a representative four-term Legendre fit (P_0,P_2,P_4,P_6), and the short dashed curve is the three-term (P_0,P_2,P_4).

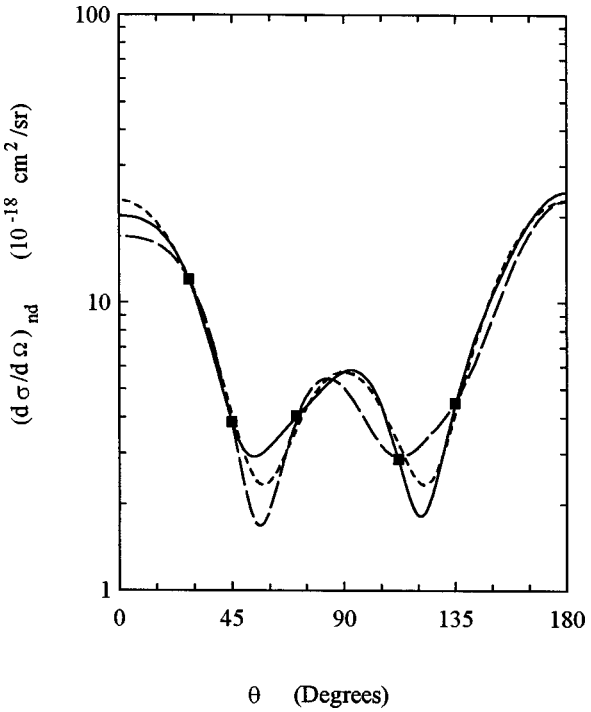

FIG. 6. The angular dependence of electrons producing neutral dissociation at 34 eV. The solid curve is a representative five-term Legendre fit (P_0,P_2,P_3,P_4,P_9), the long dashed curve is a representative four-term Legendre fit (P_0,P_2,P_4,P_7), and the short dashed curve is the three-term fit (P_0,P_2,P_4).

less than 15%. Table I shows the coefficients a_0, a_2, and a_4 of the three-term fits (P_0,P_2,P_4). Typical results of angular fits to the data for ionization at 22 eV are shown in Fig. 5, those for neutral dissociation at 34 eV are shown in Fig. 6.

Since the total dissociation cross section is the sum of the ionization cross section and the neutral dissociation cross section, the consistency of the inelastic data could be tested (i.e., does the sum of angle integrated ionization and neutral dissociation equal the angle integrated sum of the two?). Table II shows the comparison of the sum of the ionization and neutral dissociation cross sections with the directly determined total dissociation cross section.

B. Normalization to an absolute scale

Experimental values obtained by others are available for the total,[12,13] integrated elastic,[11] integrated total dissociation,[5] and integrated ionization cross sections.[7,14] We chose the recommended total cross section of Christophorou *et al.*[2] for normalization of our data for the reasons given in Ref. 8. The previously mentioned uncertainties in our ionization cross-section measurements do not affect the total cross section in a major way since the integrated ionization cross section is less than 12% of the total cross section (i.e., a 30% error in the ionization cross section translates to a less than 4% error in the total).

III. RESULTS AND CONCLUSIONS

In Fig. 1 a typical coincidence spectrum, taken at an angle of 45° and an impact energy of 34 eV, is shown. The electron impact energy loss spectrum is displayed at the top with the ions in coincidence recorded below. Accidental coincidences have been subtracted from the spectrum according to a procedure described in Ref. 9. The horizontal coincidence line labeled A corresponds to the formation of CF_3^+, B to CF_2^+, and C to CF^+. In Fig. 2 the ratio of total ion coincidence counts to total electron counts is shown as a function of electron flight time (energy loss) for 34 eV incident electrons scattered through 45°. This ratio corresponds to the absolute instrumental efficiency for ion detection.[6] The increasing noise for long electron flight times is due to a

TABLE II. Comparison of integrated cross sections obtained from various polynomial fits (unit: 10^{-16} cm^2).

Process	Energy (eV)	Four-term fits	Five-term fits
Neutral dissociation	22	0.43±0.01	0.45±0.02
	25	0.62±0.09	0.62±0.01
	34	0.71±0.06	0.75±0.06
Ionization	22	0.78±0.08	0.78±0.09
	25	1.32±0.09	1.31±0.11
	34	1.93±0.02	1.89±0.17
Total dissociation	22	1.24±0.18	1.25±0.01
	25	1.94±0.19	1.87±0.26
	34	2.69±0.15	2.66±0.16

TABLE III. Comparison of integrated cross-section measurements by different investigators (unit: 10^{-16} cm^2).

Process	Reference	22 eV	25 eV	34 eV
Neutral dissociation	Present result	0.44±0.07	0.63±0.12	0.74±0.11
	5–7	0.49±0.26	0.61±0.37	0.55±0.68
	3	0.007	0.011	0.021
Ionization	Present result	0.79±0.24	1.32±0.33	1.92±0.48
	7	0.68±0.10	1.06±0.16	2.35±0.35
Total dissociation	Present result	1.24±0.31	1.93±0.39	2.69±0.40
	5	1.17±0.23	1.67±0.33	2.90±0.58

large statistical uncertainty from the low number of events registered. The smooth dashed curve is the theoretical efficiency based on the deconvolution procedure described in Ref. 6. The matching scale factor for this theoretical curve, the instrumental efficiency, has been determined by least-squares fitting to the experimental data. Figure 4 shows a blown up portion of the inelastic energy loss spectrum shown in Fig. 1 plotted as a function of energy loss. Note that the intensity obtained by time of flight, $d\sigma/dt$, requires multiplication by the cube of the flight time for conversion to $d\sigma/dE$. The ionization contribution, obtained from the coincidence spectrum, has been placed on the same relative scale by means of the instrumental efficiency. Subtraction of the ionization from the total inelastic reveals the contribution from neutral dissociation. To obtain the total ionization cross section the apparent total ionization cross section (the number of e–ion coincident events) must be divided by two since the ionization region includes contributions from both scattered and ejected electrons. The dividing factor could be somewhat larger than two if cross sections for multiple charge ionization were appreciable in comparison to the single ionization cross sections which is not the case here because of the low impact energies used.

The coefficients, a_i, of three-term Legendre fits (P_0, P_2, P_4) for various angular-dependent cross sections are given in Table I. Since the P_0, P_2, and P_4 terms dominated in the four- and five-term Legendre fits, and the coefficients of these three terms were found to be relatively constant, the coefficients for four- and five-term Legendre expansions are not included in Table I. The results from fitting the angular differential cross sections to various four- and five-term Legendre functions are given in Table II. The uncertainties are the standard deviation of all fitting results. Additional uncertainties are discussed below. It is obvious that the integrated cross sections are relatively independent of the fit and that the sum of neutral dissociation and the ionization cross sections add up to the total dissociation cross section in each case.

In Table III the results obtained in this study are compared to those obtained by other investigators. The estimated uncertainties in our results take into account the uncertainties in the normalizing data (CF_4 total cross section and He elastic cross sections), statistical uncertainty from number of events observed, estimated uncertainty in determining the detector efficiencies, and the uncertainty introduced by the use of different fitting functions to obtain integrated cross sections.

In Table III, the entry ''5–7'' for ''neutral dissociation'' means the total dissociation results of Winters and Inokuti[5] with the ion component given in Ref. 7 subtracted out. The entry ''3'' for ''Neutral dissociation'' is obtained by summing the direct measurement of the electron energy dependence of the partial cross section for dissociation of CF_4 into neutral CF_3, CF_2, and CF radicals.[3] The values represent an estimate of the total cross section for electron impact dissociation for neutral species. It is obvious that they are inconsistent with the values of the entry ''5–7'' and those of ''present result.''

The most accurately determined inelastic cross sections in our experiments are the total dissociation and the neutral dissociation cross sections. This is because of the large uncertainty in determination of the ionization contribution at high energy loss (small scattered electron energy). The total ionization cross section is in agreement with the measurements reported in Ref. 7 to within our error estimate.

In summary, we have applied a recently reported indirect method for determining the integrated cross sections for neutral dissociation to CF_4. The integrated cross sections for elastic, total dissociation and ionization obtained in this experiment are in agreement with previously published literature values for these quantities. The agreement between our neutral dissociation cross sections and the inferred results of Winters and Inokuti[5] are all within the uncertainties assigned to each value. The reason for serious disagreement between our neutral dissociation cross sections and those of Sugai *et al.*[3] is unclear. It does not seem reasonable that the only remaining unobserved neutral fragment, atomic carbon, in the direct measurement of Sugai *et al.*[3] should be able to explain the large deviations. The energy dependence of Sugai *et al.*'s measurements does not appear to match those of other works. This would make it appear that the disagreement is due to something other than a problem with the scale factor.

[1] R. A. Bonham, Jpn. J. Appl. Phys., Part 1 **33**, 4157 (1994).
[2] L. G. Christophorou, J. K. Olthoff, and M. V. V. S. Rao, J. Phys. Chem. Ref. Data **25**, 1341 (1996).
[3] H. Sugai, H. Toyoda, T. Nakano, and M. Goto, Contrib. Plasma Phys. **35**, 415 (1995).
[4] P. C. Cosby, J. Chem. Phys. **98**, 9544 (1993).
[5] H. F. Winters and M. Inokuti, Phys. Rev. A **25**, 1420 (1982).
[6] M. R. Bruce and R. A. Bonham, J. Mol. Struct. **352/353**, 235 (1995).
[7] M. R. Bruce and R. A. Bonham, Int. J. Mass Spectrom. Ion Processes **123**, 97 (1993).
[8] L. Mi and R. A. Bonham, J. Chem. Phys. **108**, 1904 (1998), preceding paper.
[9] M. R. Bruce, L. Mi, C. R. Sporleder, and R. A. Bonham, J. Phys. B **27**, 5773 (1994).
[10] M. J. Brunger, S. J. Buckman, L. J. Allen, I. E. McCarthy, and K. Ratnavelu, J. Phys. B **25**, 1823 (1992).
[11] L. Boesten, H. Tanaka, A. Kobayashi, M. A. Dillon, and M. Kimura, J. Phys. B **25**, 1607 (1992).
[12] R. K. Jones, J. Chem. Phys. **84**, 813 (1986).
[13] C. Szmytkowski, A. M. Krzysztofowicz, P. Janicki, and L. Rosenthal, Chem. Phys. Lett. **199**, 191 (1992).
[14] H. U. Poll, C. Winkler, D. Margreiter, V. Gill, and T. Märk, Int. J. Mass Spectrom. Ion Processes **112**, 1 (1992).